Thermal properties of methyltrimethoxysilane aerogel thin films

Leandro N. Acquaroli,[1,a] Pascal Newby,[2] Clara Santato,[1]
and Yves-Alain Peter[1,b]
[1]*Department of Engineering Physics, Polytechnique Montreal, P.O. Box 6079, Station Centre-Ville, Montreal, Québec H3C 3A7, Canada*
[2]*Department of Mechanical Engineering, Université de Sherbrooke, 3000 Bv. Université, Sherbrooke, Québec J1K 0A5, Canada*

(Received 28 July 2016; accepted 8 October 2016; published online 17 October 2016)

Aerogels are light and porous solids whose properties, largely determined by their nanostructure, are useful in a wide range of applications, e.g., thermal insulation. In this work, as-deposited and thermally treated air-filled silica aerogel thin films synthesized using the sol-gel method were studied for their thermal properties using the 3-omega technique, at ambient conditions. The thermal conductivity and diffusivity were found to increase as the porosity of the aerogel decreased. Thermally treated films show a clear reduction in thermal conductivity compared with that of as-deposited films, likely due to an increase of porosity. The smallest thermal conductivity and diffusivity found for our aerogels were 0.019 W m^{-1} K^{-1} and 9.8 × 10^{-9} m^2 s^{-1}. A model was used to identify the components (solid, gaseous and radiative) of the total thermal conductivity of the aerogel. [http://dx.doi.org/10.1063/1.4965921]

I. INTRODUCTION

Silica aerogels exhibit low density (≈100 kg m^{-3}), porosity between 80% and 99.8%, pore sizes in the range of nanometers (≈15 nm), high specific surface area (≈1000 m^2 g^{-1}), very low thermal conductivity (≈0.01 W m^{-1} K^{-1}), optical transparency in the visible spectrum (¿85%), low refractive index (1.05) and superhydrophobicity.[1,2] Their properties have attracted attention due to their wide range of applications, such as in thermal and acoustic insulation,[1] kinetic energy absorption,[3] fiber optics[4] and antireflection coatings.[5]

Silica aerogels can be easily synthesized in monoliths, grains, powders and films via sol-gel,[2,6] using common precursors such as tetramethyl orthosilicate (TMOS) and tetraethyl orthosilicate (TEOS), following a critical point drying process. To reduce costs and synthesis complexity, aerogels have been fabricated in ambient conditions using, for instance, TEOS with a silylation process[7–9] or a dedicated precursor such as methyltrimethoxysilane (MTMS).[5,10,11] Both methods produce aerogels covered with methyl groups, providing hydrophobic behavior which prevents the possible collapse of the aerogel that might occur upon drying. Silylation is based on the introduction of silyl groups in the aerogel surface before drying, while MTMS precursors yield aerogels in ambient conditions without any modification, since their molecular structure[11] (Fig. S1 in the supplementary material), including methyl groups, provides hydrophobicity[5,10] and mechanical flexibility[12] to the aerogel. The 3-omega method has been used extensively for measuring the thermal conductivity and diffusivity of isotropic and anisotropic thin films, bulk materials,[13] porous films[7,14,15] and multilayer stacks.[16,17]

Here, we report on the thermal conductivity and diffusivity of MTMS-based aerogels obtained using the 3-omega method in ambient conditions. Based on their compatibility, different percentages

[a]Electronic mail: leandro-nicolas.acquaroli@polymtl.ca
[b]Electronic mail: yves-alain.peter@polymtl.ca

of TEOS and TMOS (as co-precursors) were mixed with MTMS, to explore the possibility of controlling the structural, optical and thermal properties of the aerogel. Finally, a thermal conductivity vs. density model was used to describe the contribution of the solid particles, the gas inside the pores and the radiative components of the aerogel to the total thermal conductivity.

II. EXPERIMENTAL DETAILS

The fabrication of silica aerogel films was carried out in a two-step sol-gel procedure. All chemicals were purchased from Sigma-Aldrich and used as received. The main precursor for the aerogel syntheses was MTMS, with TMOS or TEOS as co-precursors. Syntheses were performed at room temperature and pressure using the following procedure:[5,10,18] $(0.5 - x)$ mL MTMS + x mL TMOS or TEOS (where $x = 0, 5, 12.5, 25, 37.5, 50$ μL for TMOS, and $x = 0, 50, 100, 150$ μL for TEOS, giving a total volume of 0.5 mL + 4.87 mL of MeOH + 0.25 mL of 10 mM oxalic acid were dissolved and stirred for 30 min, then left to rest for hydrolysis during 24 h. Then, 0.31 mL of 11.2 M NH_4OH (aq) was added and the new solution, stirred for 15 min, was sealed to prevent evaporation and for condensation and aging for 48 h. The result was a gel with alcohol-filled pores (alcogel).[1] After addition of MeOH the alcogel was sonicated at 20 kHz, to obtain a homogenized solution. Then, films were obtained by spin-coating the homogenized solutions on thermally grown SiO_2 substrates at 2000 rpm for 40 s, providing complete substrate coverage and negligible edge effects (Fig. S2 in the supplementary material). The effect of thermal treatment was also studied by thermally drying the aerogel films at 450 °C for 1 h after deposition.

Structural analysis of the aerogels was performed using an ESEM Quanta 200 FEG Scanning Electron Microscope (SEM), a white light optical profiler Fogale Nanotech Photomap 3D and a Vecco Dektak 150 profilometer. Optical characterization was carried out using a variable angle spectroscopic ellipsometer RC2 (from 190 nm to 1700 nm) and an infrared spectrometer from J. A. Woollam Co. Inc.

The 3-omega method was set up to determine the thermal properties of the aerogel films.[13,19–21] Conventional lithography was used to pattern the top contact pads. A 200 nm thick SiO_2 capping layer was sputtered, using an RF magnetron sputtering tool. This avoided penetration of the pores.[7] Then, Au was deposited by e-beam evaporation to produce the metal contacts for heating and thermometry7 (Fig. S3 in the supplementary material). The driving current was supplied by a Keithley 6221 AC source. First (1ω) and third (3ω) harmonic voltages frequency responses were detected with lock-in Signal Recovery 7265. The thermal coefficient of resistance (c_{tr}) was determined from the resistance-temperature evolution, obtained by setting a temperature ramp with a Peltier stage between 15 °C and 60 °C and recording the 4-point probe resistance with an Agilent 3458a digital multimeter.

III. RESULTS AND DISCUSSIONS

The behavior of the film porosity, thickness and roughness for different TMOS v/v%[22] in the synthesis was investigated first (Fig. 1). A comparison of the thicknesses obtained with profilometry and ellipsometry is presented in Fig. S4(a) in the supplementary material. The porosity and the refractive index values of the aerogels were calculated from ellipsometry spectra using the effective medium theory considering the aerogel as a composite of air and silica.[5,10,23,24] The porosity was obtained using the relation $(1.399 - n_{aerogel})/(1.399 - n_{air})$, where $n_{aerogel}$ and n_{air} are the refractive indexes of the aerogel (Fig. 1(a)) and air, respectively, and 1.399 indicates the refractive index of the non-porous aerogel.[5]

It was found that the higher the TMOS v/v% the lower the porosity, whereas the thickness shows its minimum value at 5 v/v%, and a maximum at 0 v/v% TMOS (Fig. 1(b)). The root mean squared (RMS) roughness of the films was found to decrease as the TMOS v/v% increased, with a quasi-plateau for TMOS v/v% values higher than 5% (Fig. 1(c)). This behavior of the roughness parameter is in agreement with that of the porosity, considering that lower porosities induce lower roughness.[25] For aerogels synthesized with TEOS, the porosity shows similar trends. The thickness decreases as the TEOS percentage increases, and the roughness

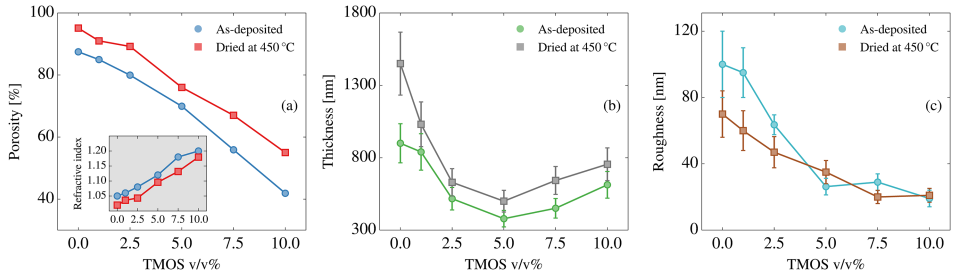

FIG. 1. (a) Porosity, (b) thickness, and (c) RMS roughness of as-deposited and thermally treated aerogel films fabricated with MTMS and different TMOS v/v%. Inset of (a): refractive index (at $\lambda = 550$ nm) vs. TMOS v/v%. Lines are visual guides.

stabilizes, after a considerable drop, when TEOS reaches 20 v/v% (Figs. S4(b) and S5 in the supplementary material). SEM images confirmed smoother aerogel surfaces in the presence of TMOS (Fig. 2).[5,7,10,18,26,27]

A set of aerogel films was thermally treated after deposition to study the effects of this process on the thermal properties of the films. First, an optimization was performed to determine the optimal temperature for the thermal treatment. Three similar aerogel samples were dried at 200 °C, 300 °C and 450 °C, where the best performance was found at 450 °C, in agreement with other works.[5,7–10] Thermally treated samples at 450 °C show higher porosity and thickness, as well as smoother surfaces (Fig. 1). The increase of the thickness can be explained in terms of the spring-back effect taking place in the aerogels after the initial shrinkage associated with the drying process.[5,7–10]

FTIR spectra were measured to determine the chemical composition of the aerogels with different percentages of TMOS and TEOS. One of the advantages of using the MTMS precursor is the presence of the non-hydrolyzable methyl groups on the aerogel surface[5,10] (Fig. 3). These groups make the aerogels hydrophobic and, thus, prevent their collapse upon drying. As the TMOS v/v% is increased, the Si–CH3 contributions at 790 cm^{-1} (rocking mode) and 1275 cm^{-1} (symmetrical deformation mode) decrease[26,28,29] and films become more hydrophilic.[5,10] An analogous effect is observed with TEOS precursor (Fig. S6 in the supplementary material).

The thermal properties of the aerogel films were characterized using the 3-omega technique. The transformations of the measured 1ω and 3ω voltages into temperature spectra were performed taking into account the half-width (b) and length (l) of the Au line, and the thermal coefficient of resistance (c_{tr}).[30] The thermal conductivity and diffusivity were then obtained by fitting the measured temperature spectra with the heat-conduction model for thin film multilayers developed by Borca-Tasciuc, assuming the aerogel films act as isotropic materials. Including heat conduction effects inside the heater, the heater's temperature rise is given by:[13]

$$T_{h,2\omega} = \frac{T_{2\omega}}{1 + i\,4\,\omega\,(\rho_h\,c_h\,d_h)\left(\frac{bl}{p}\right)T_{2\omega}} \tag{1}$$

where $T_{2\omega}$ is the temperature change without taking into account heater effects, p is the peak electrical power, ω is the angular frequency, $(\rho_h\,c_h)$ and d_h, the heat capacitance and thickness of the heater.

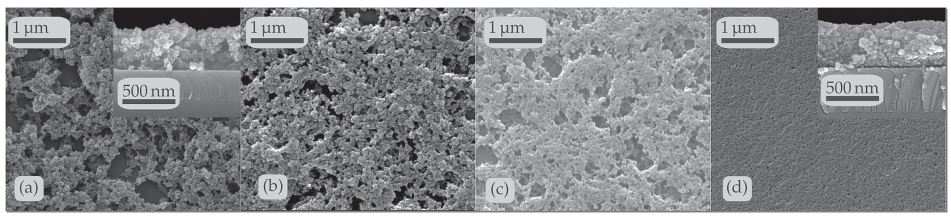

FIG. 2. SEM images of as-deposited aerogels: (a) 100 v/v% MTMS aerogel; inset: cross-section of the aerogel film; (b) Aerogel with 2.5 v/v% TMOS; (c) Aerogel with 5 v/v% TMOS, (d) Aerogel with 10 v/v% TMOS; inset: cross-section of the aerogel film.

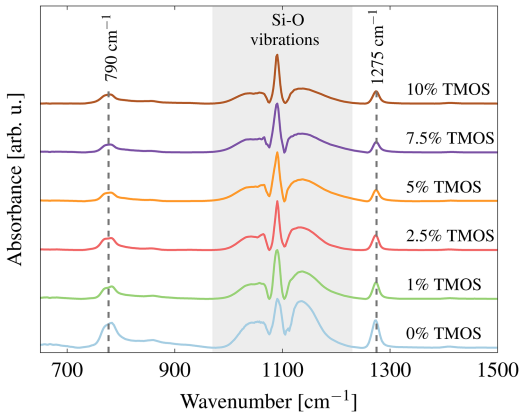

FIG. 3. Absorbance FTIR spectra of the MTMS aerogel films synthesized with different TMOS v/v%. The shaded area around 1100 cm^{-1} shows typical Si–O contributions in silica aerogels, while bands at 790 cm^{-1} and 1275 cm^{-1} are associated to the Si–CH3 related modes.

The setup was validated (Figs. S7–S9 in the supplementary material). In order to characterize each aerogel film, a four-layer system was configured: sputtered SiO_2 (≈200 nm thick)/aerogel film/thermal SiO_2 (≈200 nm thick)/Si wafer (525 μm thick). The thermal conductivity and diffusivity of thermal and sputtered SiO_2 layers, as determined with the 3-omega setup, were 1.499 W m^{-1} K^{-1} and 7.59 ×10^{-7} m^2 s^{-1}, for the thermal SiO_2, and 1.024 W m^{-1} K^{-1} and 6.70 × 10^{-7} m^2 s^{-1} for the sputtered SiO_2, in agreement with previous works.[31–34] The silicon wafer's parameters were taken from literature.[35] The thermal conductivity and diffusivity of the MTMS aerogel were obtained using the Borca-Tasciuc model for different TMOS v/v% (Fig. 4). Temperature-frequency spectra show excellent agreement with theoretical fits (Fig. S7 in the supplementary material). It was found that the higher the TMOS v/v% the larger is the thermal conductivity, attributable to the decrease of porosity. The thermal diffusivity ranges between 10^{-8}-10^{-7} m^2 s^{-1}. Similar behavior was found for aerogels based on TEOS (Fig. S10 in the supplementary material).

The thermal conductivity and diffusivity of thermally treated aerogels increase as the porosity decreases, following the same tendency of non-treated samples. However, the thermal treatment reduces the thermal conductivity with the lowest value observed being 0.019 W m^{-1} K^{-1} (Fig. 4(a)). This is 20% lower than that of air at standard conditions of temperature and pressure (0.026 W m^{-1} K^{-1}).[36] Furthermore, it is one of the lowest thermal conductivity values for non-silylated and air-filled (non-evacuated) MTMS-based aerogel films, synthesized at ambient conditions.[1,7,8] The thermal diffusivity also decreases after thermal treatment (Fig. 4(b)).

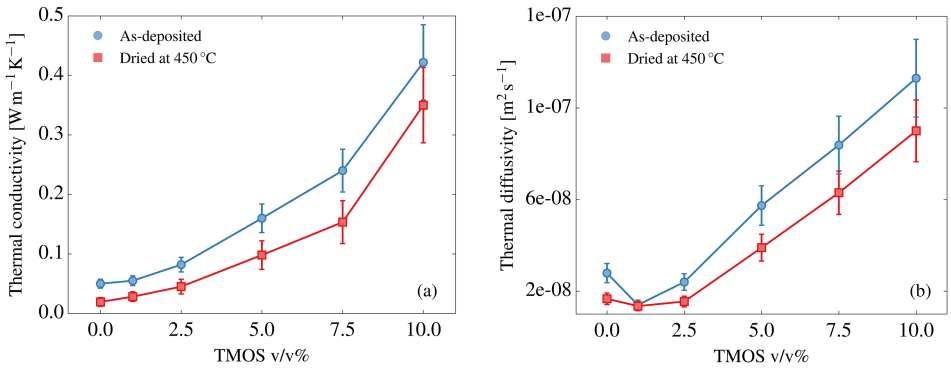

FIG. 4. Thermal conductivity (a) and diffusivity (b) of as-deposited and thermally treated MTMS aerogel films fabricated with different TMOS v/v%. Lines are visual guides.

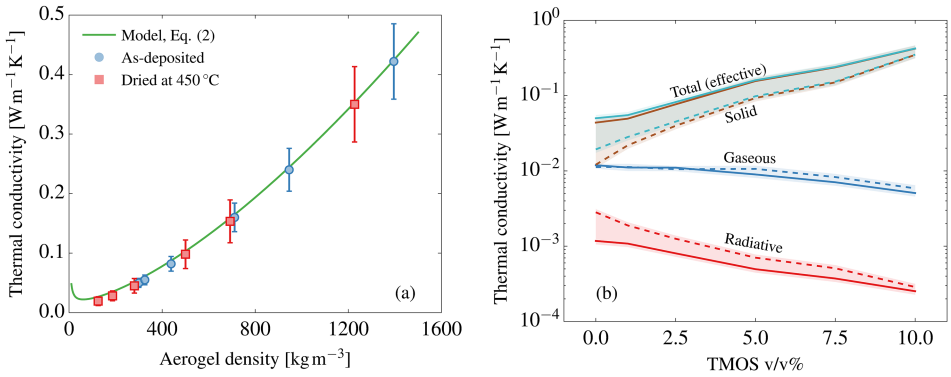

FIG. 5. (a) Thermal conductivity vs density evolution of the as-deposited and thermally dried MTMS aerogel films fabricated with different TMOS v/v%. The continuous line represents the model (Eqs. (2)). (b) Contributions of the solid (Eq. (2a)), gas (Eq. (2b)) and radiative (Eq. (2c)) phases to the total thermal conductivity. Continuous lines correspond to the as deposited samples and dashed lines to thermally treated samples.

The thermal conductivity of non-evacuated aerogels can be described by the conduction through the small solid particles, k_s, and the gas inside the pores, k_g, and the radiation, k_r:[37]

$$k_s = \rho_{aerogel}\, v_{aerogel}\, [k_{SiO_2}/\rho_{SiO_2}\, v_{SiO_2}] \tag{2a}$$

$$k_g = (k_{g,0}\, \Pi)/(1 + 2\, K_n) \tag{2b}$$

$$k_r = (16\, n^2\, \sigma\, T^3)/(3\, \rho_{aerogel}\, \kappa_{SiO_2}/\rho_{SiO_2}) \tag{2c}$$

where k_{SiO_2}, ρ_{SiO_2}, v_{SiO_2} and κ_{SiO_2} denote the thermal conductivity, the density, the sound velocity and the extinction coefficient of silica, respectively, Π, n and $\rho_{aerogel}$ are the porosity, effective refractive index, density and the sound velocity of the aerogel, respectively, k_{g0} the thermal conductivity of still free air at standard conditions of pressure and temperature, K_n the Knudsen number, σ the Boltzmann constant, and T the temperature inside the material. Taking the porosity and the refractive index of the aerogels from Fig. 1, and the other parameters indicated in Eqs. (2) from the literature[37–39] ($v_s = 5900\ m s^{-1}$, $p_s = 2200\ kg\ m^{-3}$, $k_s = 1.34\ W\ m^{-1}\ K^{-1}$, $k_{g,0} = 0.026\ W\ m^{-1}\ K^{-1}$, $\alpha = 2$, $n = 1$, $\sigma = 5.67 \times 10^{-8}\ W\ m^{-2}\ K^{-4}$, $K_s = 22.7$), the relationship between thermal conductivity and density was plotted, both for the as-deposited and the thermally dried aerogels (Fig. 5(a)). The smallest density value obtained was 110 kg m^{-3}, for a thermally dried aerogel with 0 v/v% TMOS. In the low density region, the thermal conductivity exhibited a slight deviation from the model, attributable to limited validity of the model assumptions and the hypothesis that the aerogel is exclusively made of silica. The contributions to the thermal conductivity were calculated from Eqs. (2), and are shown in Fig. 5(b). The largest contribution to the thermal conductivity comes from the solid phase (silica particles); this contribution significantly decreases after thermal treatment as a consequence of the lower density. The gaseous phase contribution is one order of magnitude smaller than that of the solid phase. The thermal treatment of the aerogels has a negligible effect on the gas phase contribution. The radiative component, as a consequence of the low mass fraction and the large surface area of silica aerogels,[37] together with the fact that experiments were performed at room temperature (Eqs. (2)), has a negligible contribution. An increase of the radiative contribution is observed for samples thermally dried after deposition, probably due to the smaller values of the density. Smaller particle sizes decrease the radiative component by raising the complexity of the solid path in the aerogel network, reducing the gas flow and creating a larger number of interfaces that act as barriers to the propagation of thermal radiation.[40] The same analysis on aerogel films including TEOS shows a similar behavior (Figs. S11 and S12 in the supplementary material). Particle size were estimated from SEM images for the TMOS precursor aerogels at 0, 2.5, 5 and 10 v/v%, yielding about 28.9, 33, 44 and 53 nm for the as-deposited aerogels, and about 16, 30, 23 and 41 nm for the thermally treated ones, respectively. As expected from the thermal conductivity behavior of the aerogels, it is possible to conclude the smaller particle sizes induce a decrease in the porosity.[16,40–42]

IV. CONCLUSIONS

Aerogel thin films based on MTMS were synthesized and their functional properties investigated at standard temperature and pressure conditions. The structural optical and thermal properties of the aerogels were modified by inclusion of TMOS and TEOS as co-precursors during synthesis.

The porosity and roughness of the films were found to decrease with the increase of the v/v% of TMOS and TEOS, whereas the film thickness shows a minimum for 5 v/v% TMOS, and decreases monotonically for TEOS. Significant increases in the porosity (up to 8%) and thickness (up to 50%) were observed for thermally treated films. The increase in the thickness was attributed to an enhanced spring-back effect, inducing greater porosity.

The thermal conductivity of the aerogels was found to increase quasi-linearly with the co-precursor v/v%. This is probably associated with the porosity since higher porosity implies lower conductivity. The same trend was observed for the thermal diffusivity of the films. Films after thermal treatment exhibited lower thermal conductivity and diffusivity compared with those of the as-deposited films: the smallest values reached for non-evacuated and non-silylated aerogels were 0.019 W m^{-1} K^{-1} (20% lower than that of air at standard conditions of temperature and pressure, 0.026 W m^{-1} K^{-1}) and 9.8×10^{-9} m^2 s^{-1}, respectively.

Employing a simple density model, the solid, gaseous and radiative thermal contributions to the total thermal conductivity of the aerogels were studied. The solid phase contribution is greatest, one order of magnitude more than that of the gaseous phase. The radiative contribution was found to be negligible. Particle size were found to increase with larger amounts of TMOS v/v% in the mixture. It can also be stated that the lowest values of thermal conductivity are observed for aerogels with the smaller particle sizes. Work is in progress to deduce the particle sizes in TEOS aerogels and the results will be object of a further publication. A thorough understanding of the effect of nanostructure sizes and features, such as inter-particle contacts, could be studied by analyzing the behavior of thermal conductivity over a wide range of pressures and temperatures, where effects such as solid-gas coupling can be used to reveal the structure of the material.[1,41,43,44]

SUPPLEMENTARY MATERIAL

See the supplementary material for further details about the molecular structure of MTMS, aerogel homogenized solutions, 3ω setup and validation, and results for TEOS co-precuror.

ACKNOWLEDGMENTS

L.N.A. thanks to Dr. Jérémy Maxin for discussions on the 3-omega setup. This work was supported by the National Science and Engineering Research Council of Canada (NSERC).

[1] M. A. Aegerter, N. Leventis, and M. M. Koebel. (Eds.), *Aerogels Handbook* (Springer, New York, 2011).
[2] N. Bheekhun, A. R. A. Talib, and M. R. Hassan, "Aerogels in aerospace: An overview," Adv. Mater. Sci. Eng. **2013**, 406065.
[3] P. C. Thapliyal and K. Singh, "Aerogels as promising thermal insulating materials: An overview," J. Mater. **2014**, 127049.
[4] M. D. W. Grogan, "Aerogel and fibre optics," Ph.D. thesis, Department of Physics, University of Bath (2010).
[5] A. Yildirim, T. Khudiyev, B. Daglar, H. Budunoglu, A. K. Okyay, and M. Bayindir, "Superhydrophobic and omnidirectional antireflective surfaces from nanostructured ormosil colloids," ACS Appl. Mater. & Interfaces **5**, 853 (2013).
[6] X. Guo, Q. Zhang, X. Ding, Q. Shen, C. Wu, L. Zhang, and H. Yang, "Synthesis and application of several sol–gel-derived materials via sol–gel process combining with other technologies: A review," J. Sol-Gel Sci. Tech. **1** (2016).
[7] M. L. Bauer, C. M. Bauer, M. C. Fish, R. E. Matthews, G. T. Garner, A. W. Litchenberger, and P. M. Norris, "Thin-film aerogel thermal conductivity measurements via 3ω ," J. Non-Cryst. Solids **357**, 2960 (2011).
[8] S. S. Prakash, C. J. Brinker, A. J. Hurd, and S. M. Rao, "Silica aerogel films prepared at ambient pressure by using surface derivatization to induce reversible drying shrinkage," Nature **374**, 439 (1995).
[9] S. S. Prakash, C. J. Brinker, and A. J. Hurd, "Silica aerogel films at ambient pressure," J. Non-Cryst. Solids **190**, 264 (1995).
[10] H. Budunoglu, A. Yildirim, M. O. Guler, and M. Bayindir, "Highly transparent, flexible, and thermally stable superhydrophobic ormosil aerogel thin films," ACS Appl. Mater. & Interfaces **3**, 539 (2011).
[11] A. V. Rao, S. D. Bhagat, H. Hirashima, and G. M. Pajonk, "Synthesis of flexible silica aerogels using methyltrimethoxysilane (MTMS) precursor," J. Colloid Interface Sci. **300**, 279 (2006).
[12] T. Matias, C. Varino, H. C. de Sousa, M. E. M. Braga, A. Portugal, J. F. J. Coelho, and L. Durães, "Novel flexible, hybrid aerogels with vinyl- and methyltrimethoxysilane in the underlying silica structure," J. Mat. Sci. **51**, 6781–6792 (2016).
[13] T. Borca-Tasciuc, A. R. Kumar, and G. Chen, "Data reduction in 3ω method for thin-film thermal conductivity determination," Rev. Sci. Instrum. **72**, 2139 (2001).

[14] D.-A. Borca-Tasciuc and G. Chen, "Anisotropic thermal properties of nanochanneled alumina templates," J. Appl. Phys. **97**, 084303 (2005).
[15] M. M. Rojo, J. Martin, S. Grauby, T. Borca-Tasciuc, S. Dilhaire, and M. Martin-Gonzalez, "Decrease in thermal conductivity in polymeric P3HT nanowires by size-reduction induced by crystal orientation: New approaches towards thermal transport engineering of organic materials," Nanoscale **6**, 7858 (2014).
[16] T. Borca-Tasciuc, W. Liu, J. Liu, T. Zeng, D. W. Song, C. D. Moore, G. Chen, K. L. Wang, M. S. Goorsky, T. Radetic, R. Gronsky, T. Koga, and M. S. Dresselhaus, "Thermal conductivity of symmetrically strained Si/Ge superlattices," Superlattices Microst. **28**, 199 (2000).
[17] M. Mazumder, T. Borca-Tasciuc, S. C. Teehan, E. Stinzianni, H. Efstathiadis, and S. Solovyov, "Temperature dependent thermal conductivity of Si/SiC amorphous multilayer films," Appl. Phys. Let. **96**, 093103 (2010).
[18] Z. Li, X. Cheng, S. He, D. Huang, H. Bi, and H. Yang, "Preparation of ambient pressure dried MTMS/TEOS co-precursor silica aerogel by adjusting NH_4OH concentration," Mat. Let. **129**, 12 (2014).
[19] D. G. Cahill, M. Katiyar, and J. R. Abelson, "Thermal conductivity of a-Si:H thin films," Phys. Rev. B **50**, 6077–6081 (1994).
[20] C. Dames and G. Chen, "1ω , 2ω , and 3ω methods for measurements of thermal properties," Rev. Sci. Instrum. **76** (2005).
[21] T. Tong and A. Majumdar, "Reexamining the 3-omega technique for thin film thermal characterization," Rev. Sci. Instrum. **77** (2006).
[22] TMOS v/v% is defined as: [vol. TMOS / (vol. TMOS + vol. MTMS)] * 100. The same relation applies for TEOS.
[23] L. N. Acquaroli, R. Urteaga, and R. R. Koropecki, "Innovative design for optical porous silicon gas sensor," Sens. Actuator B-Chem. **149**, 189 (2010).
[24] L. N. Acquaroli, R. Urteaga, C. L. A. Berli, and R. R. Koropecki, "Capillary filling in nanostructured porous silicon," Langmuir **27**, 2067 (2011).
[25] B. Bessaïs, *Handbook of porous silicon* (Springer International Publishing, Cham, 2014) Chap. Ultrathin Porous Silicon Films, p. 1.
[26] S. V. Ingale, P. B. Wagh, A. K. Tripathi, V. S. Kamble, R. Kumar, and S. C. Gupta, "Physico-chemical properties of silica aerogels prepared from TMOS/MTMS mixtures," J. Porous Mater. **18**, 567 (2010).
[27] H. E. Rassy, P. Buisson, B. Bouali, A. Perrard, and A. C. Pierre, "Surface characterization of silica aerogels with different proportions of hydrophobic groups, dried by the CO_2 supercritical method," Langmuir **19**, 358 (2003).
[28] H. E. Rassy and A. C. Pierre, "NMR and IR spectroscopy of silica aerogels with different hydrophobic characteristics," J. Non-Cryst. Solids **351**, 1603 (2005).
[29] R. Al-Oweini and H. El-Rassy, "Synthesis and characterization by FTIR spectroscopy of silica aerogels prepared using several $Si(OR)_4$ and $R"Si(OR')_3$ precursors," J. Mol. Struct. **919**, 140 (2009).
[30] C. Dames, "Measuring the thermal conductivity of thin films: 3-omega and related electrothermal methods," in *Annual Review of Heat Transfer*, Vol. **16** (Begell House Digital Library, 2013) Chap. 2.
[31] *Thermal Conductivity. Theory, Properties, and Applications*, edited by T. M. Tritt (Kluwer Academic Plenum Publishers, New York, 2004).
[32] T. Yamane, N. Nagai, S.-I. Katayama, and M. Todoki, "Measurement of thermal conductivity of silicon dioxide thin films using a 3ω method," J. Appl. Phys. **91**, 9772 (2002).
[33] A. S. Grove, *Physics and Technology of Semiconductor Devices* (Wiley, 1967).
[34] S.-M. Lee, D. G. Cahill, and T. H. Allen, "Thermal conductivity of sputtered oxide films," Phys. Rev. B **52**, 253 (1995).
[35] H. R. Shanks, P. D. Maycock, P. H. Sidles, and G. C. Danielson, "Thermal conductivity of silicon from 300 to 1400 K," Phys. Rev. **130**, 1743 (1963).
[36] J.-J. Zhao, Y.-Y. Duan, X.-D. Wang, and B.-X. Wang, "Effects of solid-gas coupling and pore and particle microstructures on the effective gaseous thermal conductivity in aerogels," J. Nanopart. Res. **14**, 1 (2012).
[37] L. W. Hrubesh and R. W. Pekala, "Thermal properties of organic and inorganic aerogels," J. Mater. Res. **9**, 731 (1994).
[38] X. Lu, M. C. Arduini-Schuster, J. Kuhn, O. Nilsson, J. Fricke, and R. W. Pekala, "Thermal conductivity of monolithic organic aerogels," Science **255**, 971 (1992).
[39] X. Lu, R. Caps, J. Fricke, C. T. Alviso, and R. W. Pekala, "Correlation between structure and thermal conductivity of organic aerogels," J. Non-Crys. Solids **188**, 226 (1995).
[40] X. Zheng, L. Qiu, G. Su, D. Tang, Y. Liao, and Y. Chen, "Thermal conductivity and thermal diffusivity of SiO_2 nanopowder," J. Nanopart. Res. **13**, 6887 (2011).
[41] D. G. Cahill, P. V. Braun, G. Chen, D. R. Clarke, S. Fan, K. E. Goodson, P. Keblinski, W. P. King, G. D. Mahan, A. Majumdar, H. J. Maris, S. R. Phillpot, E. Pop, and L. Shi, "Nanoscale thermal transport. II. 2003–2012," Appl. Phys. Rev. **1**, 011305 (2014).
[42] H. Dong, B. Wen, and R. Melnik, "Relative importance of grain boundaries and size effects in thermal conductivity of nanocrystalline materials," Scientific Reports **4**, 7037 (2014).
[43] H. Liu, Z.-Y. Li, X.-P. Zhao, and W.-Q. Tao, "Study on unit cell models and the effective thermal conductivities of silica aerogel," J. Nanosci. Nanotechnol. **15**, 3218 (2015).
[44] A. Bernasconi, T. Sleator, D. Posselt, J. K. Kjems, and H. R. Ott, "Dynamic properties of silica aerogels as deduced from specific-heat and thermal-conductivity measurements," Phys. Rev. B **45**, 10363 (1992).